Analysis and optimization of a wideband metamaterial absorber made of composite materials

Olivier Rance, Anne Claire Lepage, Xavier Begaud, Michel Soiron, André Barka, Patrick Parneix

APPLIED PHYSICS A – EXTENSION FROM META 2018 CONFERENCE PAPER "WIDEBAND METAMATERIAL ABSORBER MADE OF COMPOSITE MATERIALS"

Analysis and Optimization of a Wideband Metamaterial Absorber Made of Composite Materials

Olivier Rance[1], Anne Claire Lepage[1], Xavier Begaud[1], Michel Soiron[2], André Barka[3], and Patrick Parneix[4]

[1]LTCI, Télécom ParisTech, Université Paris-Saclay, France
[2]SART, France
[3]ONERA/DEMR, Université de Toulouse, France
[4]Naval Group, France
*corresponding author, E-mail: olivier.rance@telecom-paristech.fr

Abstract

Using structural composite materials for the fabrication of Radar Absorbing Materials (RAM) allows combining the strong load bearing capability with the radar absorbing functionality in a unique structure. This article shows the possibility to transpose an already existing metamaterial absorber to the domain of composite materials. The dielectric layers of the absorber initially designed with radio-frequency (RF) materials are replaced with fiber-reinforced composite materials classically used for naval applications that have been specially manufactured and characterized. The working principle of the absorber is explained in detail by analyzing the influence of each layer on the Smith chart. The performances of the re-optimized composite absorber are compared against the initial RF design and against other classical absorbers. The composite design has a total thickness of 8.9 mm and achieves a reflection coefficient below -14 dB within the band 4.6 GHz - 17.2 GHz at normal incidence. The reflection coefficient remains under -10 dB at oblique incidence up to 45°.

1. Introduction

RAM have been traditionally used for stealth purposes in the military domain. Lately they have become of great interest also for solving electromagnetic interference problems in aerospace and civil domains.

The consortium set up under the SAFASNAV project aims to develop an innovative structural composite panel concept for use on naval platforms. The high level of stealth requirements for military ships pushes the development of new technologies, particularly in terms of materials limiting the reflectivity of radar waves. At the same time, superstructures (topsides) become complex metasystems integrating a large number of sensors, and generating delicate problems of electromagnetic compatibility.

Composite materials have a key role to play in dealing with these new issues, both because they are materials that are perfectly adapted to the naval environment, as nearly half a century of operation on all oceans has shown but also because they can be multifunctional materials capable of performing a structural role, as well as other functions., in particular for the realization of electromagnetic (EM) absorbers [1].

There are several approaches for designing radar absorbing structures. A classical solution, called Salisbury screen [2], consists in a resistive sheet mounted a quarter-wavelength apart from a ground plane. The extension of the Salisbury screen to multiple resistive sheets is called the Jaumann absorber [3]. The screens are separated by dielectric slabs of about a quarter wavelength thickness. Jaumann absorbers achieve wider bandwidth but at the cost of the thickness. A way to improve the performances of the previous absorbers is to replace the purely resistive sheets by resistively loaded frequency selective surfaces (FSS). In this manner it is possible either to reduce the thickness of the structure like in metamaterial absorbers [4] or to improve the bandwidth like in analog circuit absorbers [5].

In this paper, we consider a wideband metamaterial absorber which has been initially designed with RF materials [6]. We replace the dielectric layers by structural composite materials from the naval domain that have been specially manufactured and measured. The different thicknesses of the composite layers are re-optimized to evaluate the performance that can be achieved with these new materials.

The paper is organized as follows: The second section is a quick overview of the absorber and of the equivalent model used for the optimization. The measured EM characteristics of the composite materials are also detailed in this section. The third section includes the analysis of the absorber by use of Smith chart. The benefit of the FSS compared to purely resistive sheets is emphasized. The performances obtained with composite materials are then compared to the original design in the last paragraph.

This work is a part of the development of an ultra-wide bandwidth absorber of low thickness realized within the framework of the SAFASNAV project.

2. Absorber

The absorber under study has been designed in the framework of a previous project called SAFAS (Self-complementary surface with low signature) [6], [7]. It is

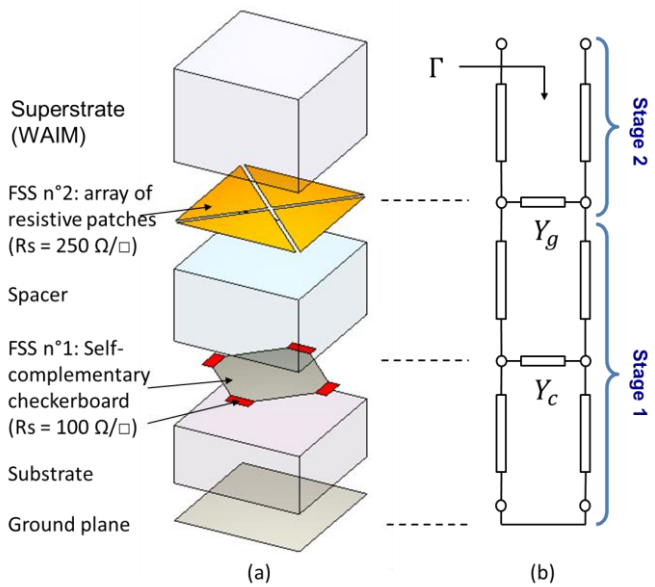

Figure 1: (a) Geometry of the unit cell and (b) equivalent circuit of the EM absorber.

composed of three dielectric layers separated by two FSS, which are located above a ground plane (Fig.1-a).

The permittivity of the initial RF dielectric layers (Superstrate, Spacer, Substrate in Fig.1-a) were 2.2, 2.3 and 4.3 respectively [6]. These RF materials are replaced by structural composite laminates classically used in the naval domain for large structural panel fabrication. They have been manufactured using the industrial vacuum infusion molding process which is illustrated by a picture in Fig. 2. The permittivity of these materials has been measured at

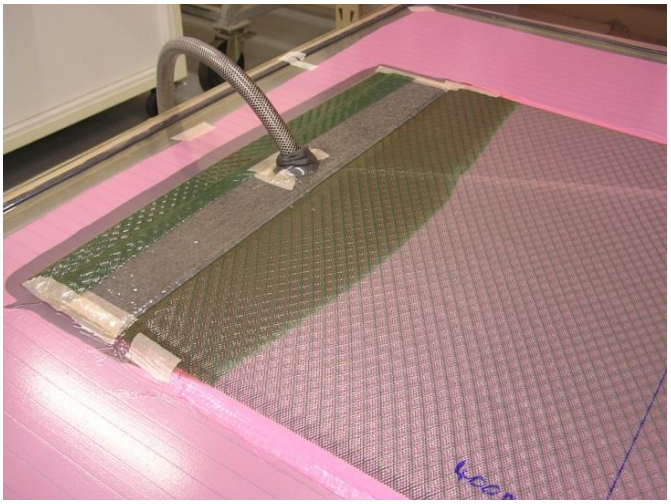

Figure 2: Manufacturing of composite dielectric panel by the industrial vacuum infusion molding process.

Table 1: EM characteristics of composite layers

Layer	Superstrate	Spacer	Substrate
Reinforcement	Quartz	S-glass	E-glass
Resin	Vinylester	Vinylester	Polyester
Permittivity	3.1	4	4.7
Loss tangent	0.02	0.02	0.02

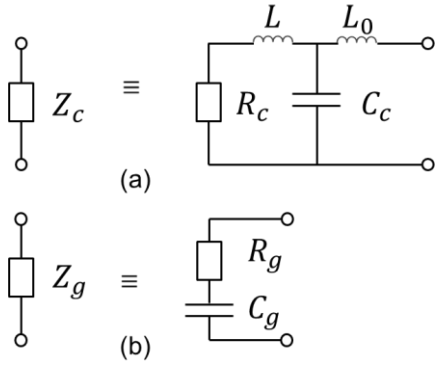

Figure 3: (a) Equivalent circuit of the FSS n°1: self-complementary checkerboard loaded with resistive element. (b) Equivalent circuit of the FSS n°2: array of resistive patches.

ONERA using CAREM and BACCARAT bench. The composition and associated EM characteristics of these composite are given in Table 1. Compared to the RF materials, we note a significant increase of the permittivity for all layers. The loss tangent is also more important for the first two layers but this does not impact the behavior of the absorber.

This absorber can be modeled by an equivalent circuit which is represented in Fig.1-b. Each dielectric layer is associated to a transmission line section and the thin FSS are associated to their admittances.

The equivalent circuits of the first FSS (loaded self-complementary checkerboard) [8] and of the second FSS (array of resistive patches) [9] are given in Fig.3-a, and Fig.3-b respectively. The cascading of the ABCD matrices of each layer allows calculating in a very efficient manner the reflection coefficient of the whole structure [9]. The equivalent model is used to rapidly analyze and optimize the absorber with calculation tools like Matlab. The optimized result is checked against Full-Wave simulations (CST Microwave Studio) in a second step.

3. Operating principle

In the SAFAS study [6], the concept of the absorber has been validated by measurement but no in-depth analysis of the absorber has been performed. In this section the absorber is analyzed layer by layer with the Smith chart. The structure of the absorber can be broken down into two functional stages which are depicted graphically in Fig. 1. The first stage achieves both wideband adaptation and wide-angle stabilization while the second stage further extends the bandwidth.

3.1. First stage analysis

The first stage is composed of a grounded dielectric substrate, a self-complementary checkerboard loaded with resistive elements (FSS n°1), and a dielectric spacer. The total thickness of the first stage is 5.2 mm. The admittance of each layer separately as well as the total admittance of

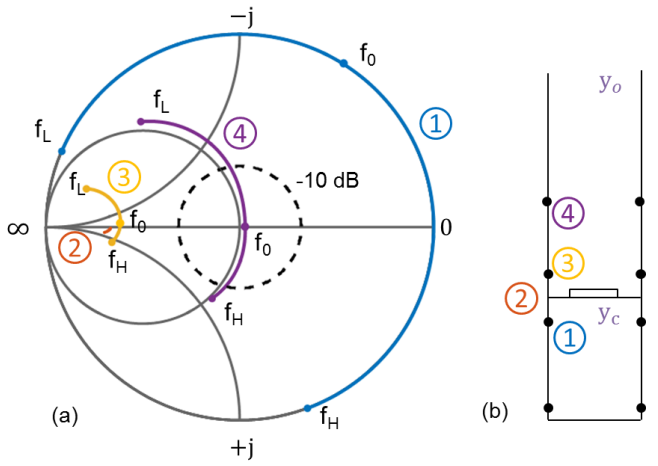

Figure 4: (a) Admittance of the first stage layer by layer. The Smith chart is normalized with respect to free space admittance. The circled numbers correspond to the admittance seen at the location marked in (b). ① is the admittance of the shunt, ② is the admittance of the freestanding FSS, ③ is the complex sum of ① and ②, and ④ is the total admittance of the first stage.

stage 1 are indicated in the admittance Smith chart normalized with respect to free space admittance in Fig. 4. The goal for the matching process is to get as close as possible to the center of the Smith chart.

The admittance of the ground plane plus substrate ① is equivalent to the one of a shunted transmission line and is thus inductive (upper part of the circle) at low frequency f_L and becomes capacitive (lower part of the circle) for high frequency f_H. The Smith chart shows that the freestanding loaded self-complementary checkerboard ② is intrinsically wideband as similar to a point in the circle. It is also slightly capacitive, which compensates the inductive component of the shunt at f_0. In other terms, the addition of the loaded checkerboard above the grounded substrate enables the point corresponding to f_0 to go from inductive in ① to the real axis in ③. The curve is then brought back to the center of the Smith chart ④ by the transmission line (TL) section corresponding to the spacer.

In order to show the benefit of this design, the performance of the first stage ④ is compared against classical Salisbury absorbers in Fig. 5. The first Salisbury screen (Fig. 5-a) is composed of air dielectric and has a thickness of 5.2 mm. The second Salisbury screen (Fig.5-c) is composed of a dielectric whose permittivity is equal to the Spacer layer $\varepsilon_r = 4$ and has a thickness of 3 mm. At normal incidence, SAFASNAV absorber, despite its high permittivity, exhibits a band very similar to the Salisbury screen with air dielectric (-10 dB between 8 GHz and 17 GHz), and much wider than the high permittivity Salisbury screen (-10 dB between 10 GHz and 15 GHz). Considering oblique incidence, the Salisbury screen with air dielectric exhibits an important frequency shift for increasing angle (approximately 4 GHz at 45°). This shift is limited for the other designs (+500MHz at 45°) due to the high permittivity dielectrics. We also see that the increase of the reflection coefficient with respect to the angle is less pronounced for SAFASNAV absorber (-12.5 dB at 45°) than for the two Salisbury screens (-10 dB at 45°).

3.2. Second stage analysis

The second stage is composed of an array of resistive patches realized with a resistive film (FSS n°2) and a dielectric superstrate playing the role of a Wide Angle Impedance Matching (WAIM) layer. The reflection coefficient of each element is represented on the admittance Smith chart in Fig. 6.

The freestanding FSS is capacitive ⑤ which helps to compensate the inductive behavior of stage 1 at low frequency ④, resulting in a curve ⑥ which is almost symmetric with respect to the real axis of the chart. The TL section corresponding to the WAIM dielectric layer rotates curve ⑥ into curve ⑦. Choosing this separation to be

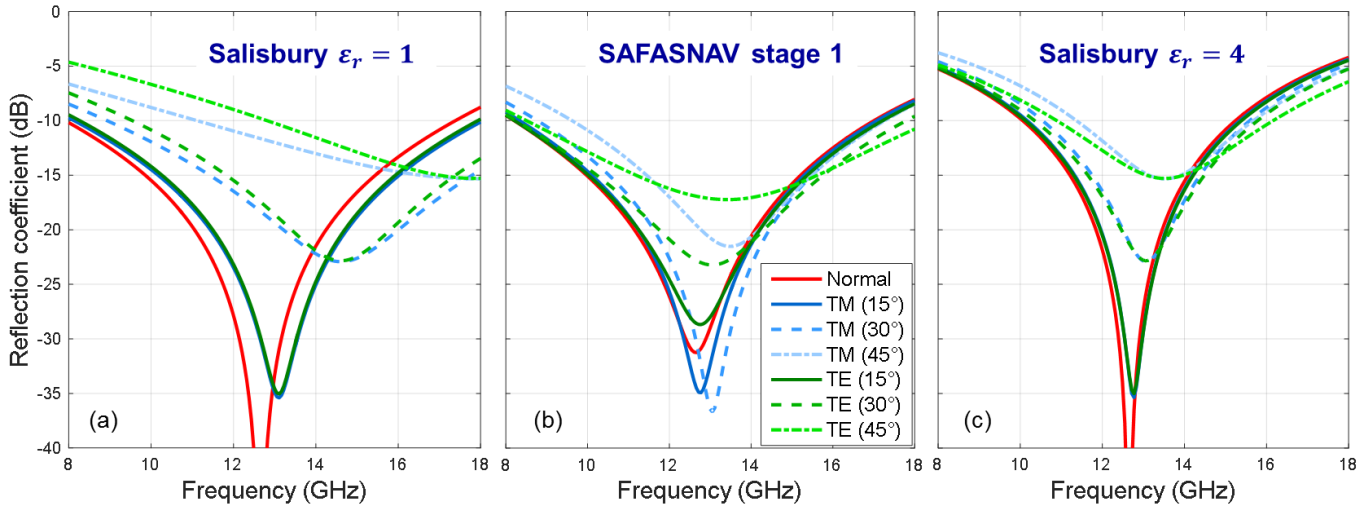

Figure 5: Reflection coefficient with respect to frequency for various angle of incidence. (a) Salisbury with air dielectric. (b) First stage of the SAFASNAV absorber. (c) Salisbury with dielectric having a permittivity of 4.

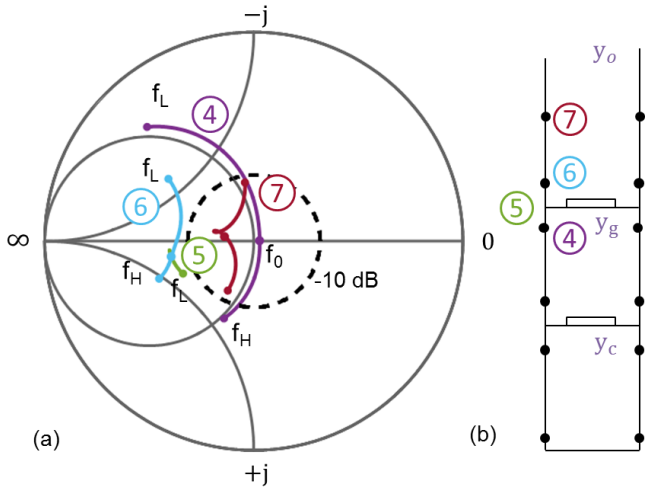

Figure 6: (a) Admittance of the second stage layer by layer. The circled numbers correspond to the reflection coefficient seen at the location marked in (b). ④ is the admittance of stage 1, ⑤ is the admittance of the freestanding resistive patch array, ⑥ is the complex sum of ④ and ⑤, and ⑦ is the total admittance of the second stage.

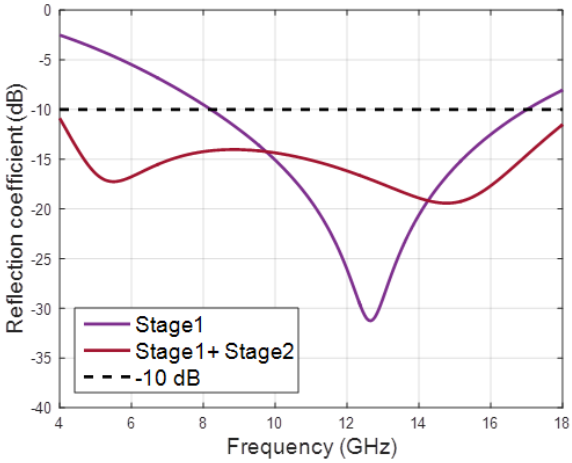

Figure 7: Reflection coefficient after the first and the second stage of the SAFASNAV absorber.

approximately λ/4 at the center frequency, we will rotate less than 180° at the lower frequency f_L and more at the higher frequency f_H. The result is the apparition of a loop on the Smith chart, and the frequencies f_L, f_0, and f_H are more clustered together in curve ⑦ than in curve ④. The reflection coefficients of stage 1 and stage 2 (corresponding respectively to ④ and ⑦ on the Smith chart) are finally compared in Fig. 7. We see that the addition of the second stage has allowed achieving an ultra-wideband response but at the cost of the level of the reflection coefficient.

4. Comparison between structural composite materials and RF materials

The optimization results (Matlab) obtained after replacement of the dielectrics by the structural materials are presented in Fig.8 and are validated by comparison with CST simulation (frequency domain solver with Floquet

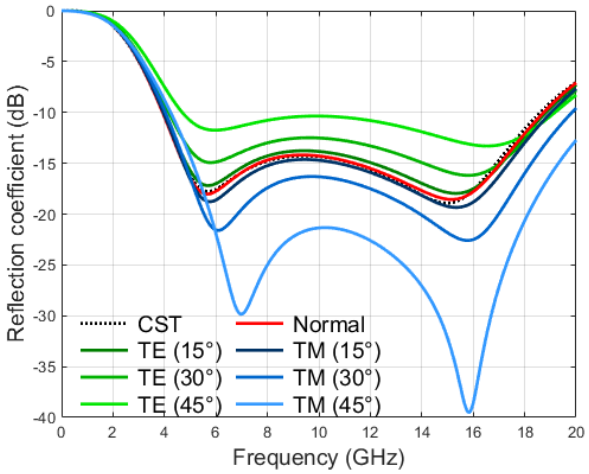

Figure 8: Reflection coefficient with respect to frequency for different angle of incidence, SAFASNAV.

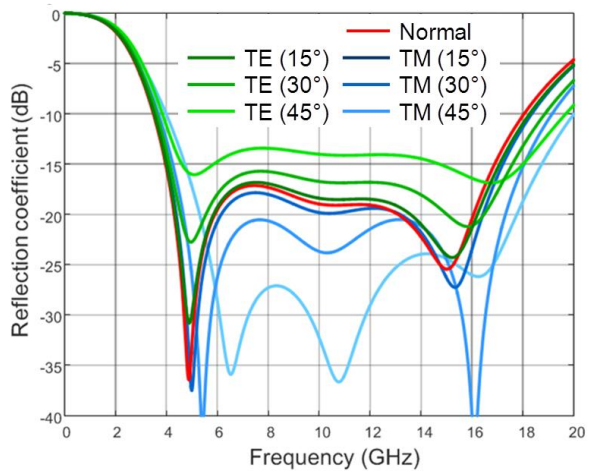

Figure 9: Reflection coefficient with respect to frequency for different angle of incidence, initial SAFAS design.

boundary conditions) at normal incidence. The analytical model is in very good agreement with the full wave simulation. The total thickness of the absorber is 8.9 mm. The reflection coefficient is less than -14 dB in the band 4.6 GHz -17.2 GHz at normal incidence. At oblique incidence, the reflection coefficient remains under -10 dB for the frequency band 5GHz to 18 GHz, for an angle up to 45°.

In order to evaluate the impact of the replacement of the RF dielectrics by structural composite materials, the results obtained in the initial design are represented in Fig 9. The two designs are showing a similar behavior with respect to angle of incidence. The reflection coefficient is increased by 4 dB between the initial SAFAS design and SAFASNAV. Finally, SAFASNAV (8.9 mm) is sensibly thinner than the initial SAFAS design (11.5 mm) which is due to the use of high dielectrics substrates.

5. Conclusions

A metamaterial absorber initially designed for RF materials has been successfully optimized with composite materials. The magnitude of the reflection coefficient is

below -14 dB within the frequency band going from 4.6 GHz to 17.2 GHz at normal incidence. It remains under -10 dB for a similar bandwidth up to 45°. This study shows that fiber-reinforced composite materials used in combination with frequency selective surfaces can be employed to design a thin and wideband structural absorber.

Acknowledgments

The research leading to these results has received funding by French Ministry of Defense (DGA), through the French National Research Agency (ANR) and Astrid Program in the framework of SAFASNAV project.

References

[1] C. Wang, M. Chen, H. Lei, K. Yao, H. Li, W. Wen, D. Fang, « Radar stealth and mechanical properties of a broadband radar absorbing structure », *Compos. Part B Eng.*, vol. 123, p. 19-27, August 2017.

[2] W. W. Salisbury, « Absorbent body for electromagnetic waves », US2599944A, 10-June-1952.

[3] L. J. du Toit, « The design of Jaumann absorbers », *IEEE Antennas Propag. Mag.*, vol. 36, nº 6, p. 17-25, Dec. 1994.

[4] N. Engheta, « Thin absorbing screens using metamaterial surfaces », in *IEEE Antennas and Propagation Society International Symposium (IEEE Cat. No.02CH37313)*, 2002, vol. 2, p. 392-395.

[5] B. A. Munk, *Frequency Selective Surfaces – Theory and Design*. New York: Wiley-Blackwell, 2000.

[6] X. Begaud, S. Varault, A. Lepage, M. Soiron, and A. Barka, « Design of a Thin Ultra Wideband Metamaterial Absorber», *Proc. of the 2017 International Conference on Electromagnetics in Advanced Applications (ICEAA)*, Verona, Italy,2017

[7] S. Varault, M. Soiron, A. Barka, A. C. Lepage, and X. Begaud, « RCS Reduction With a Dual Polarized Self-Complementary Connected Array Antenna », *IEEE Trans. Antennas Propag.*, vol. 65, nº 2, p. 567-575, Feb. 2017.

[8] O. Luukkonen, C. Simovski, G. Granet, G. Goussetis, D. Lioubtchenko, A. V. Räisänen and S. A. Tretyakov , « Simple and Accurate Analytical Model of Planar Grids and High-Impedance Surfaces Comprising Metal Strips or Patches », *IEEE Trans. Antennas Propag.*, vol. 56, nº 6, p. 1624-1632, June 2008.

[9] X. Begaud, F. Linot, M. Soiron, and C. Renard, « Analytical model of a self-complementary connected antenna array on high impedance surface », *Appl. Phys. A*, vol. 115, nº 2, p. 517-522, May 2014.